Form Approved
OMB No. 0704-0188

AD-A266 353

2. REPORT DATE
17 June 1993

3. REPORT TYPE AND DATES COVERED
Reprint

4. TITLE AND SUBTITLE
Scattering Functions Near the Sun by Large Aerosols

5. FUNDING NUMBERS
PE   61102F
PR   2310
TA   G1
WU   18

6. AUTHOR(S)
Frederic E. Volz

7. PERFORMING ORGANIZATION NAME(S) AND ADDRESS(ES)
Phillips Lab/GPOS
29 Randolph Road
Hanscom AFB, MA 01731-3010

DTIC
SELECTE
JUN 2 2 1993
B

8. PERFORMING ORGANIZATION REPORT NUMBER
PL-TR-93-2129

9. SPONSORING/MONITORING AGENCY NAME(S) AND ADDRESS(ES)

10. SPONSORING/MONITORING AGENCY REPORT NUMBER

11. SUPPLEMENTARY NOTES
Reprinted from Applied Optics, Vol. 32, No. 15, 20 May 1993

12a. DISTRIBUTION/AVAILABILITY STATEMENT

Approved for public release; Distribution unlimited

12b. DISTRIBUTION CODE

13. ABSTRACT (Maximum 200 words)

In the course of a lengthy series of observations since 1975, a large, continuous decrease of the brightness of the solar aureole has been found west of Boston, at Hanscom Air Force Base and at Lexington, Mass.   This points to the virtual disappearance from the lower atmosphere of giant particles larger than ~10 μm in size while total suspended particulates in Boston and other U.S. cities have barely decreased.   Results of calculations to better understand the relation between forward scattering and aerosol mass distribution [coarse fraction (CF)] are presented.   In addition, a method to modify steep scattering functions calculated for a plane-wave source (Sun treated as a star) to those of the actual (and limb-darkened) Sun is presented.   The calculated wavelength dependence of extinction, which is lower than that observed, is found to be little affected by the CF, but seems, like forward scattering, to be sensitive to mass distribution of sizes of <0.4 and ~0.6 μm because of the anomal scattering behavior of spheres.

14. SUBJECT TERMS Solar aureole, Aerosols,giant, Scattering functions, Aerosol size distributions, Forward scattering, Air pollution, Limb darkening, solar, Climatological change, Aerosol monitoring, PM-10 Extinction

15. NUMBER OF PAGES
7

16. PRICE CODE

17. SECURITY CLASSIFICATION OF REPORT	18. SECURITY CLASSIFICATION OF THIS PAGE	19. SECURITY CLASSIFICATION OF ABSTRACT	20. LIMITATION OF ABSTRACT
UNCLASSIFIED	UNCLASSIFIED	UNCLASSIFIED	SAR

NSN 7540-01-280-5500

Standard Form 298 (Rev. 2-89)
Prescribed by ANSI Std. Z39-18
298-102

Scattering functions near the Sun by large aerosols

93-13947

Frederic E. Volz

In the course of a lengthy series of observations since 1975, a large, continuous decrease of the brightness of the solar aureole has been found west of Boston, at Hanscom Air Force Base and at Lexington, Mass. This points to the virtual disappearance from the lower atmosphere of giant particles larger than ~ 10 μm in size while total suspended particulates in Boston and other U.S. cities have barely decreased. Results of calculations to better understand the relation between forward scattering and aerosol mass distribution [coarse fraction (CF)] are presented. In addition, a method to modify steep scattering functions calculated for a plane-wave source (Sun treated as a star) to those of the actual (and limb-darkened) Sun is presented. The calculated wavelength dependence of extinction, which is lower than that observed, is found to be little affected by the CF, but seems, like forward scattering, to be sensitive to mass distribution of sizes of < 0.4 and ~ 0.6 μm because of the anomal scattering behavior of spheres.

93 6 21 049

1. Introduction

Over most of the globe, the sky brightness close to the Sun, the aureole, is generally high because of the presence of giant particles (GP), dust of ~ 10–200-μm diameter. Over the continents, GP from the ground or from industrial activity and sometimes pollen grains from forest trees are carried upwards by turbulence and thermal convection. However, the largest GP, including pollen, may fall back to the surface during the night.

Measuring aureoles at angles < 0.10° from the Sun by a photometer or a camera is difficult; diffraction from apertures can be eliminated only by coronagraphic setups. But the brightness of aureoles and their changes can be studied by a simple method: Standing at the very edge of the shadow of a roof at least 5 m away, one determines which step of a graded set of neutral-density (ND) filters just prevents glare of the sky at the Sun's edge.[1] The ND value of this step designates the strength of the aureole. Care must be taken in order that the adaptation of the eye to moderate outside brightness does not change. Related psychological measurements were discussed by Holladay[2] and others.[3,4] While there generally is

The author is with Phillips Laboratory, Geophysics Directorate, U.S. Air Force, Hanscom Air Force Base, Massachusetts 01731-3010.

no glare (ND = 0) 2°–4° from the Sun, persistent values of ND of ~ 2.0 (and sometimes much higher) have been observed earlier by the author at the solar rim at many locations in the U.S. and in Central Europe, both in cities and in the countryside.

2. Decline of Aureole Brightness

The observations and the meteorological and environmental aspects of the results obtained during my 15-year aureole study are being reported in some detail elsewhere.[5] They will be discussed here only briefly as an introduction to scattering calculations that relate to problems posed by the observations.

Continuous observations were begun in 1974 at Phillips Laboratory, Hanscom Air Force Base (and during weekends in Lexington, Mass.), ~ 10 km to the west of Boston. Excluded from this study are much narrower, generally much brighter, and fast-changing aureoles that are due to cirrus or ice crystals from supercooled water clouds. (Indeed, the method would be useful to detect invisible cirrus.) Day-to-day and diurnal variations of aureole brightness can be significant, as shown in Fig. 1. Average annual ND values were initially 1.5. In May, pollen caused average ND's of 2, and on windy summer days, fibers as well as stellate hairs from leaves of forest trees contributed to forward scattering.

The downward trend of the ND, in both background and extreme values, was realized in 1983, convincing me to continue and even intensify the observations. Indeed, cases with no enhanced bright-
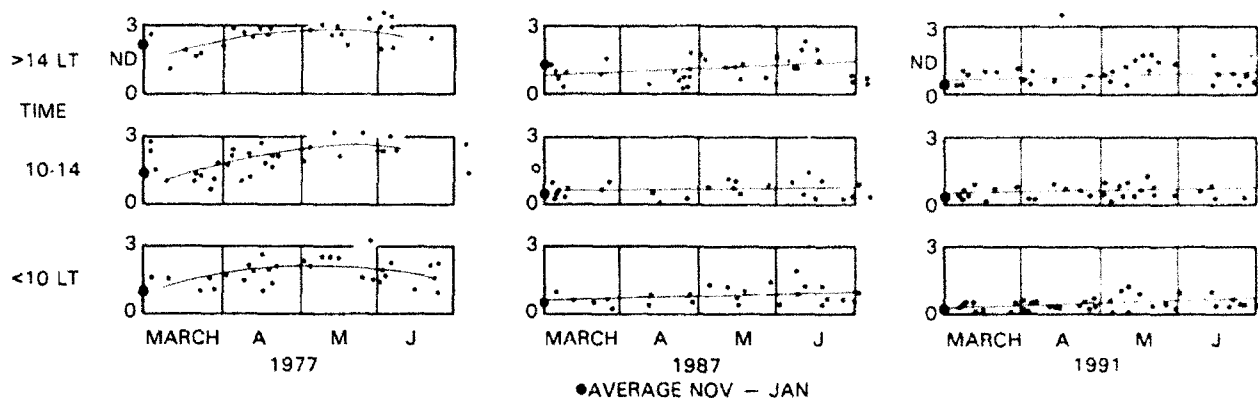
Fig. 1. Individual aureole observations from March to June, for 1977 (left), for 1987 (center), and for 1991 (right). Ordinate is ND; brightness goes from 1 (no glare) to 1000. Bottom panels are for morning hours, and top panels are for afternoon. Heavy dots at left of the panels denote averages for the periods November to January. Data are for an aerosol optical thickness (AOT) of < 0.25, but ND's for higher turbidities are similar.

ness near the Sun, i.e., an apparent lack of GP, have become more and more frequent in recent years.

The arrival in October 1991 of the stratospheric veil of Pinatubo aerosol (with an AOT of ~0.2) doubled the brightness of the sky background within 10° of the Sun. Brightness enhancement close to the sun was virtually absent, even during afternoons (suggesting that convection was more damped because of the veil), until pollen appeared the following May.

Since aureoles observed at or after noontime, when it became windy, often indicate advection from distances of 100 to more than 500 km, one must conclude that both day-to-day features and decline are not local phenomena but are representative of a large region.

The data show that the (linear) reduction of aureole brightness (or of the vertical load of GP) between 1977 and 1980 was ~35% per year and after 1980 was at least 15% annually. In contrast, precipitation chemistry[6] and sampling of total suspended particulates (TSP) by high-volume filter samplers in cities in the late 1980's showed reductions in the eastern part of the U.S. of, at the most, 6% per year[7] while visibility degradation[8] ceased and TSP in Massachusetts (from Ref. 9 and my evaluations mentioned below) did not really change.

However, the aureole data are a strong proof that GP decreased by possibly more than a factor of 100, which shows, at least in part, the success of environmental cleanup efforts in regard to coarse dust, such as that from power plants and industry. However, there are strong indications that coarse street dust stirred up by cars on highways and in cities also makes a significant contribution to GP, but it is less clear how its quantity could have decreased.

3. Aerosol Mass Distributions and the Coarse Fraction

The virtual disappearance of aureoles during my observations made it desirable to try to relate them to other data that could provide information on size distributions and possibly on changes over time.

This also suggests the need to calculate scattering functions.

Indeed, simultaneous measurements from 1983 to 1986 in several U.S. cities of TSP and of inhalable particles of less than 10 μm in size, called PM-10, yielded average coarse particle fractions (CF's), which are given by

$$CF = 1 - [(PM-10)/TSP], (1)$$

of 0.5 to 0.6.[7,10,11] Such measurements were also made, from 1985 to 1990, on roofs at several sites in Massachusetts, lasting 24 h on every sixth day. Concentrating my evaluation of printouts[12] of the data on summer months, I came to the principal conclusions that:

(i) TSP and the CF generally were the same in downtown Boston and in cities located 10 to 70 km away. TSP appeared to be proportional to turbidity (sun photometry) at the Phillips Laboratory.

(ii) The CF's of sites only a few blocks apart in downtown Boston sometimes correlated well (with a range of CF's from 0.5 to 0.7).

(iii) Otherwise, the average CF was 0.6. The few data sets covering the whole period at one site do not seem to support a change in the CF.

(iv) Farther from Boston, there are indications of a lower CF. (Similar results were reported from Wisconsin[11]). At the remote Quabbien summit (300 m) in western Massachusetts, summer values averaged to 0.4, but in winter time, which is even cleaner, PM-10 were often higher than TSP, making the data suspect.

More detailed mass distributions have been measured in parallel to CF's in some cities; a typical average is the one shown as model A in Fig. 2(a).[10] However, more sporadic data from other cities, especially those made with rotating impactors during the day, have GP peaks shifted to 30 or 100 μm [model N in Fig. 2(a)]. I mention only measurements made in
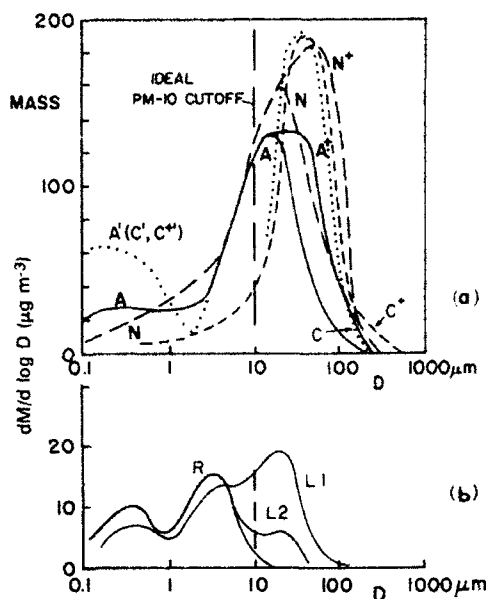
Fig. 2. Typical mass-size aerosol spectra. Areas under curves are proportional to mass. The (here idealized) 10-μm-diameter cutoff defines the CF. (a) Model A, average from Phoenix II, is typical of U.S. cities listed in Ref. 10. Model N was obtained by a rotary impactor in Seattle, Wash.[13] Model C was designed for large CF. Models A+, N+, and C+ have bigger particles than models A, N, and C, respectively. Model A' has a small-mode mass distribution that produces an anomalous extinction. (b) Models R, L1, and L2 are typical for results at rural locations[17] and from flights.[18,19]

Seattle, Wash.,[13] Chicago and Argonne, Ill.,[14] and St. Louis, Mo.[15] Most of these do not cover particles smaller than 4 μm, but the CF was most likely 0.8 or larger. The difference in the CF can partly be attributed to sample duration (24 h versus a few daytime hours). In addition, the rain hood of TSP samplers causes a premature deposit of particles ≥ 30 μm. However, all these data refer to city aerosols at busy street intersections. (In Chicago, more than of 50% of the GP appeared to come from vehicular street traffic.[16]) Indeed, for data from rural sites[17] and in flight,[18,19] the mass in the accumulation mode (size < 2 μm) and in the GP mode was approximately equal. The CF is small because few GP are larger than 10 μm [model R in Fig. 2(b)].

For the translation of these mass distributions into scattering functions, we will, for simplicity and from a lack of knowledge of vertical distributions, assume three general situations:

(i) Model N with a high CF, possibly corresponding to strong aureoles measured in the 1970's.

(ii) Model A with a CF of ~0.5, which is typical of moderate aureoles.

(iii) Flat mass distribution (model R, rural) with a low CF, which probably corresponds to the present aureole data.

Below we see that the parameterization of mass distributions by CF is also helpful for forward scattering.

However, it cannot be overlooked that rural models conflict with the recent CF data from Massachusetts. On the other hand, there are reasons, from only a few opportunities of observations, that aureoles in Boston also became weak (in the 1960's, ND readings of 2 to 3 were common). We could possibly solve these problems by assuming that the vertical extent of the cloud of coarse anthropogenic aerosol, over Boston as well as over the countryside, greatly decreased in recent years. However, this would imply an unlikely climatological change: a decrease in turbulence and convection near the surface. Yet this change could have been subtle because of the large fall speed of the large particles. An analogy is windswept snow; it settles as soon as the gust subsides. A related experience is that aureoles are always brightest on windy days, when soil might have been the main source of the dust; but why then did they also fade over the course of the years? Could it have to do with less open land and less farming?

4. Computation of Scattering Functions and Results

Calculations of scattering functions, which use the above models of size distributions, were made. But first a method is presented and later applied to derive the effect of the width of the solar disk and of limb darkening on forward-scattering calculations.

A. Effect of the Solar Disk on Scattering Functions

To relate sky brightness to variations of the vertical load and the size distribution of the GP, one must consider that the scattering function observed near the Sun is much flatter and lower than if the Sun were a point source. The closer to the Sun the observation is made and the larger the particles are, the smaller the area of the solar disk contributing to the scattering and the larger the effect of limb darkening. Thus after the calculation of a scattering function $P^*(\phi)$ (depending on the scattering angle ϕ) for a distant point source (a star), the scattering function must be converted to $P^S(\psi)$ of the Sun (the angle ψ is measured from the edge of the Sun). The function P^S is expressed as the convolution of P^* and the angular brightness distribution of the Sun.

An analytical solution of the integral exists[20] for scattering functions of the form

$$P^*(\phi) \sim c (\phi^2 + d);\qquad (2)$$

results are given in Ref. 2. For arbitrary scattering functions, linearization has been proposed.[22] Sample results of strict solutions, including limb darkening for relatively flat forward scattering, are presented in Refs. 23 and 24. However, a field of view of even less than 0.5° of a photometer may dominate the relation between P^* and P^S to up to a few degrees from the Sun.[24] This problem is irrelevant to our method of observation.

In this paper, simple algorithms derived from a graphic presentation of the scattering geometry and of the brightness distribution of the solar disk are used for the convolution. The disk is divided into
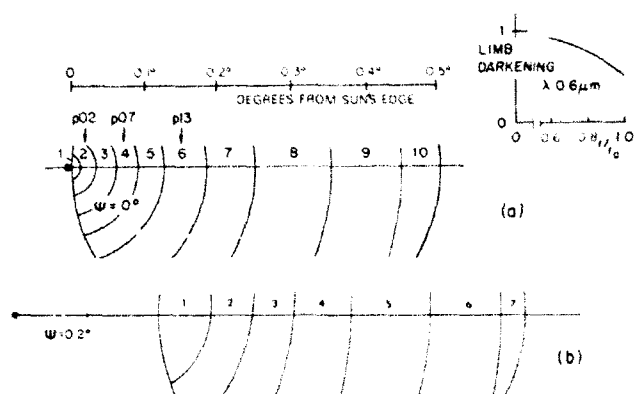
Fig. 3. Subdivision of solar disk (only partly shown) to modify the small-angle scattering function, which is caused by a distant point source, to that from the limb-darkened solar disk. (a) For observed point at edge of solar disk ($\psi = 0°$), with 10 sectors; (b) for the sky 0.2° to 1.6° from Sun. Table 1 displays the weights for the sectors and the computation scheme.

ring zones that are concentric to the respective observation points in the sky. The first evaluation, which is depicted in Fig. 3(a), is for the sky right at the edge of the Sun, where the highest accuracy is needed if the scattering function is steep. Considering that P^* is calculated in 0.1° increments of ϕ (including a value at 0.04°), P^* for an effective angle of $\phi = 0.02°$ is obtained from $[P^*(0°) P^*(0.04°)]^{1/2}$, and P^* for 0.07° and 0.13' are similarly obtained from the next pairs of primary P intensities. After taking limb darkening into consideration, we graphically determine and normalize (as for the coefficients CD in Table 1) the areas of the zones by the respective sums. The scheme for $\psi = 0.04°$ uses the same coefficients CD as for $\psi = 0°$. Simpler, but basically similar, are the evaluations for $\psi = 0.1°$, with coefficients CE. The

scheme for $\psi = 0.2°$, which uses angles ϕ to 0.7° and yields coefficients CC, is shown in Fig. 3(b). The same scheme is repeated for starting angles of $\psi = 0.3°, 0.4° \cdots 1.6°$, so that angular increments of ϕ can be (and are here) larger beyond 2.1°.

Although the errors of the coefficients (Table 1) might be as much as 3%, this is expected to cancel in the calculations. Indeed, for a P^* of constant value, P is flat to within 0.5%. Results of the method for model A can be seen in Fig. 4. The flattening, which is ~40% at the Sun's edge, obviously would be detrimental to attempts to recover by inversion the true scattering function. For particles such as ice crystals with a relatively narrow size distribution peaking at a diameter (D) of 220 μm, the edge brightness is reduced much more, to 2% only (not shown).

The validity of the scheme extends to size parameters $2\pi f * D \lambda$ of at least 1800. This follows from Eq. (3a) of Table 1 in that the intensity in the central diffraction peak should differ little at $\phi = 0.01°$ from that at $\phi = 0.0°$.

The discontinuity seen in Fig. 4 at $\psi = 1.6°$ has a simple explanation: the last modified intensity is derived from an effective angle of $\psi \approx 1.8°$, and therefore is lower than the next unmodified value at $\psi = 1.7°$. The jump is largest where the primary scattering function is steepest (solid curve). Carrying the smoothing on to larger angles will eliminate the jump.

B. Some Scattering Models

Calculations of scattering functions that use the above models of size distributions were made for particle sizes from 0.16 to 540 μm in diameter by a reliable program, although calculations for size param-

Table 1. Setup of Calculations to Convert Scattering Functions for a Starlike Sun (P^*) to those of the Actual Sun (P^S)

Primary angles ϕ for which $P^*(N)$, henceforth called $P(N)$, is assumed to have been calculated:
   0.0, 0.04, 0.1, (0.1) $\cdots$ to 2.1 deg, $[P(1)$ to $P(21)]$

Auxiliary scattering intensities and approximate angles:

$P02 = [P(1) P(2)]^{1/2}$	$\phi = 0.02°$,	(3a)
$P07 = [P(2) P(3)]^{1/2}$	$\phi = 0.07°$,	(3b)
$P13 = [P(3) P(4)]^{1/2}$	$\phi = 0.13°$,	(3c)

$P^S(1) = $ CD1 $P(1) + $ CD2 $P02 + $ CD3 $P(2) + $ CD4 $P07 + $ CD5 $P(3)$
   $+ $ CD6 $P13 + $ CD7 $P(4) + $ CD8 $P(5) + $ CD9 $P(6) + $ CD10 $P(7)$, $\psi = 0.00°$ (4a)

$P^S(2) = $ CD1 $P(2) + $ CD2 $P07 + $ CD3 $P07 + $ CD4 $P(3) + $ CD5 $P13$
   $+ $ CD6 $P(4) + $ (CD7 $+ $ CD8) $P(5) + $ CD9 $P(6) + $ CD10 $P(7)$, $\psi = 0.04°$ (4b)

$P^S(3) = $ CE1 $P(3) + $ CE2 $P13 + $ CE3 $P(4) + $ CE4 SQRT$[P(4) P(5)]$
   $+ $ CE5 $P(5) + $ CE6 $P(6) + $ CE7 $P(7) + $ CE8 $P(8)$. $\psi = 0.10°$ (4c)

$P^S(I)$ for $I = 4$ to $I = 18$:
   $P^S(I) = $ CC1 $P(I) + $ CC2 $P(I + 1) + $ CC3 $P(I + 2)$
   $+ $ CC4 $P(I + 3) + $ CC5 $P(I + 4) + $ CC6 $P(I + 5)$ $\psi = 0.2°$ to 1.6°.   (5)

Coefficients CD [for P^S at $\psi = 0.0°$ and 0.04°, Eq. (4a)]:
   0.0013, 0.072, 0.126, 0.023, 0.052, 0.119, 0.192, 0.312, 0.280, 0.045

Coefficients CE [for P^S at $\psi = 0.1$, Eq. (4b)]:
   0.0083, 0.033, 0.076, 0.130, 0.210, 0.290, 0.217, 0.030

Coefficients CC [for P^S at $\psi = 0.2$ to 1.6, Eq. (4c)]:
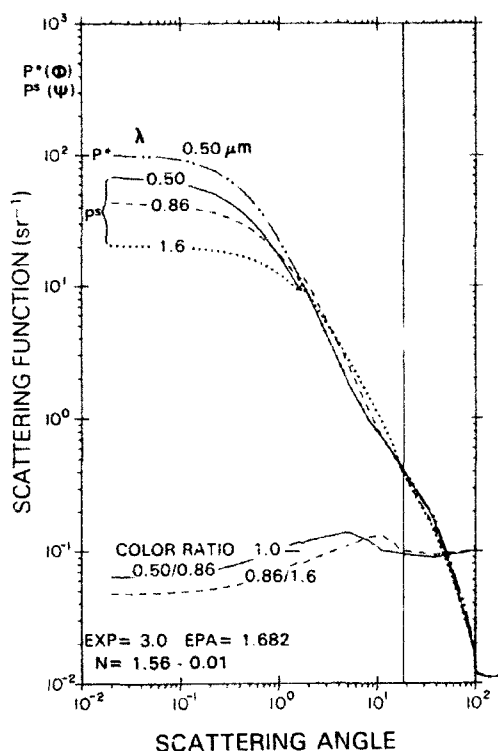   0.052, 0.192, 0.281, 0.281, 0.252, 0.032

Fig. 4. Comprehensive presentation of scattering data. Shown are scattering functions for model A at λ 0.5 μm (P^*, unmodified, and P^S modified by the solar-disk scheme), and P^S for λ 0.86 and 1.6 μm. The bottom part of the graph shows color ratios. The angles had to be increased by 0.02° for plotting. EPA is the *effective extinction cross section.* λ exponents for the λ pairs 0.86, 0.50 and 1.6, 0.86 were 0.69 and 0.58, respectively.
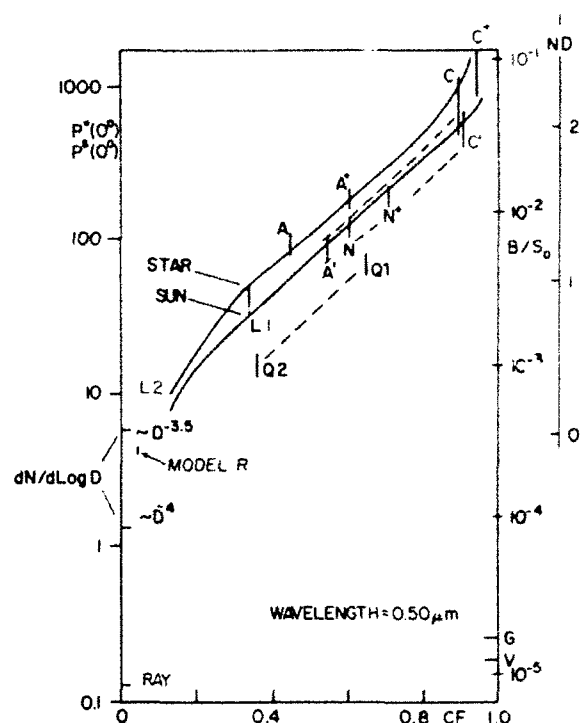

Fig. 5. Forward scattering versus CF. Normalized forward scattering P^* and P^S at the edge of the Sun for some mass distribution models of Fig. 2 are shown. The right-hand side shows ordinates for the radiance ratio of sky to Sun and for the ND, with an AOT of 0.1 and an air mass of 1.5. The upper ends of the data bars are for a starlike sun, and the lower ends are for the actual Sun. Dashed curves indicate the downshift of several models caused by mass distribution A' of their small mode. At CF $<$ 0.2, P drops off steeply to low scattering by power-law size distributions and to values marked as G and V, which was observed in the Alps[21,22]; the expected Rayleigh scattering (RAY) is indicated.

eters >500 and angles $<5°$ were usually replaced by the corresponding Bessel functions from Fraunhofer diffraction optics. The logarithmic increment (base 10) in size is 0.1. Initially, a power-law size distribution is assumed (the label EXP in Fig. 4), but specifying factors in logarithmic size increments of 0.26 will result in a logarithmically interpolated mass distribution. Calculations were usually restricted to the three wavelengths (of Fig. 4, but in the following, generally only results for λ = 0.5 μm are considered. As is appropriate for the sky near the Sun in typical situations of continental pollution, no molecular scattering was included. By remaining in the realm of normalized scattering functions, actual mass concentrations do not matter, and effects that are due to variations of the path length in the atmosphere (solar elevation angle) and aerosol extinction are neglected, as is multiple scattering. In short, the results are generally valid for small overall turbidity and the Sun near zenith.

The results of the calculations for the edge of the Sun, plotted against the CF, are shown in Fig. 5. On the right-hand side, an ordinate relating P to sky radiance B with respect to extraterrestrial radiance S_0 of the solar disk (of solid angle of 67×10^{-6} sr), has been added (e.g., Refs. 23 and 24). A typical AOT of 0.1 at λ = 0.5 μm and an air mass of 1.5 are assumed. The ND scale is based on measurements taken in a

clear sky with a high Sun: ND = 0 corresponds to $B/S_0 = 40 \times g\ 10^{-6} \pm 20\%$.

Data points obtained from models A, N, and C, and with an increase in the height or width of the GP mode (models A^+, N^+, and C^+), together with models L1, L2, and R from Fig. 2(b), are plotted against CF. P^* and P^S are shown as upper and lower ends of the data bars, respectively. For CF $>$ 0.3, brightness is $\sim 40\%$ lower for the actual Sun than for a starlike sun.

At a small CF, one must consider that scattering at 0° of power-law size distributions with the exponent -3 (which would produce a straight line in Fig. 2) or flatter distributions would rise unlimited unless a largest size is specified. For the power-law size distributions indicated in Fig. 5 (mass decreasing with increasing size), the CF is essentially zero.

The result is that log P or NDs an increase, which is proportional to the CF. Between CF $\sim$ 0.2 and 0.9, the slope d ND/d CF is $\sim$2.2.

It was also investigated how scattering by a sharp pollen peak fares if the GP part is subjected to a uniform reduction (from mass distribution Q1 to Q2 in Fig. 6), say, by fallout. This caused the CF to halve, and decreased the brightness at angles $<4°$, as
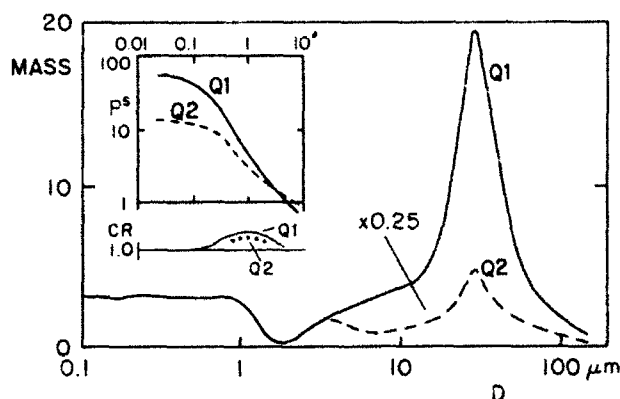
Fig. 6. Sensitivity study: Effect on scattering function P^S $(\lambda = 0.50$ μm, inset) of the reduction of a sharp GP peak (model Q1) by a factor of 0.25 (model Q2). The brightness at the Sun's edge is affected by the same factor. The color ratio $(\lambda, 0.86\ 0.50)$ of Q2 is slightly lower than for Q1.

Fig. 7. Wavelength exponents α of extinction from regular models (in the figure in the region below α = 1.0) and of A'-type models in the upper part. The solid circles indicate α between wavelengths of 0.50 and 0.86 μm and the long dashes indicate α between wavelengths of 0.86 and 1.6 μm. Observations of the exponent α deviate little from 1.3 and were found to be insensitive to aureole brightness. Models S (not mentioned above) and N do not have the usual minimum mass near sizes of ~1 μm; the model O2 has, compared with model O1, a bulge at $D = 0.6$ μm.

shown in the inset of Fig. 6. But the reduction of the brightness reflects the change of mass at the peak which attests to the dominance of scattering by the pollen. However, the color ratio of model Q2, which also peaks at 1°, is slightly lower than that of Q1. Otherwise, the sharp peak reduces the absolute scattering considerably with regard to CF (Fig. 5).

With model A, which was modified by a high number of particles at $D < 0.4$ μm (model A'), a large increase of the λ dependency of extinction and a loss of scattering at angles $< 30°$ was found. Therefore, more models (C and C*) were modified, too, at $\lambda < 0.4$ μm by the same distribution (models C' and C*'). This reduces scattering even at a high CF, as indicated by the dashed curves in Fig. 5. The effects are related to the anomalous extinction by these small particles.

Overall, these results show that neglect in our database of the shape and width of observed aureoles is not detrimental if particle mass is of prime interest.

Now, what is the relation between the model results at the Sun's edge and the ND scale on the right-hand side of Fig. 5? The agreement appears to be quite good. These attempts to get confirmation of the aureole data from scattering theory seem to indicate that the CF concept is, in general, quite helpful for the study of forward scattering by typical pollution aerosols.

5. Wavelength Dependence of Extinction

A brief look at the possibility of connecting routine Sun photometer results concerning the wavelength exponent α of aerosol extinction to aureoles is now given. This value (as usual, its absolute value) has the advantage in sampling the vertical load, as does the ND, and in referring to the place of the ND observation. The respective results for α of our regular models decrease, as seen in the lower part of Fig. 7, between wavelengths of 0.50 and 1.6 μm from about 0.9 to 0.7, as the CF goes from 0.2 to 0.9. The decrease of α to 0 (as during dust storms in the visible part of the spectrum) occurs only at much longer
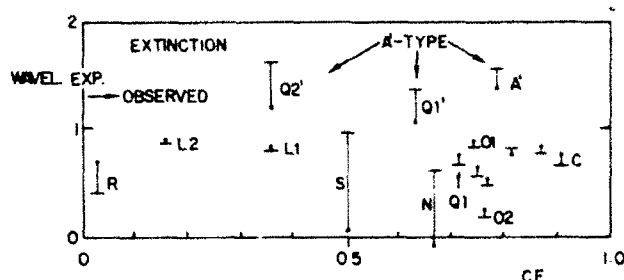
wavelengths. However, anomal extinction that is due to a large number of particles with $D < 0.4$ μm (as in model A') increases α for the considered CF's to values greater than one, fitting them into the upper part of Fig. 7.

The actual influence of GP or small particles on extinction was studied by sun photometer data at wavelengths of 0.38, 0.50, and 0.86 μm for the summers from 1976 to 1978, in the absence of volcanic turbidity. The average α being 1.3, even observations with ND > 2.7 show no smaller exponents than those with ND < 1.0, regardless of turbidity. Since the mass distributions causing anomal extinction cannot always prevail, this method also does not help to establish trends of ND. Is it that the mass distributions assumed are too structured to affect α? The problems also probably cannot be resolved by assuming that the aureole decline is reflecting the decrease of particles with $D > 30$ μm, which are known to have been missed in measurements of TSP during windy weather.

6. Summary and Conclusions

For the past sixteen years I have estimated, both at Hanscom Air Force Base and in Lexington, to the west of Boston, the brightness of the solar aureole at the edge of the Sun. My purpose was to study variations of the vertical load of giant aerosol particles. Unexpectedly, the average brightness of aureoles decreased continually until they essentially disappeared in the background of small particle scattering. However, the interrelation between the decline of the aureole brightness, for which there is no support from other evidence, and comparatively constant roof-level pollution is still not clear. To partly address this question, emphasis in this study was on calculations of forward scattering to better understand the relation of aureole brightness to typical mass–size distributions of aerosols. The calculations include the presentation and use of a method to account for the effect of the width of the solar disk and of limb darkening on forward scattering. These

effects result in flattening and lowering of scattering near the Sun, but they weaken the relationship between the shape of the scattering function and the size distribution of particles. Thus it makes observations easier but would greatly hinder efforts to invert measured scattering functions to yield size–mass distributions.

Several aerosol models have been investigated. Surprisingly, the concept of the CF (mass of particles $> 10 \mu m$/total mass) often used (in the form $1 - CF$) to characterize the results of routine monitoring by filter samplers allows one to present normalized scattering functions at the solar rim in a seemingly concise manner. That is, the CF and the glare (ND) of the aureole are closely related and are rather independent of the shape and the width of the mass distribution of the large particles. Hence the angular width, shape, and coloration of the aureole (which were neglected in the presentation of the observations) also are not important.

The models clearly show that the recent aureoles observed at Phillips Laboratory (and probably in Boston as well) are caused by low-CF mass distributions. But in 1990 roof-level values of CF ~ 0.5 were still measured in Boston, and, more relevant to aureoles at Phillips Laboratory, in cities of central and western Massachusetts. A way out of this dilemma is the assumption that the GP's are now falling out faster because of lower turbulence near the surface. And should Boston aureoles now indeed be as low as those at Phillips Laboratory, one might have to assume that the street-corner pollution is not representative of the optics of the Boston sky, or even of the whole of the Boston roof-level aerosol.

An excursion into results on the wavelength dependence of extinction reveals that the λ exponent of the regular models is only slightly affected by the CF (and the ND), but is much lower than observed. Hence it is obvious that several questions remain regarding the interplay between mass distributions, optical observations, and modeling.

References

1. F. E. Volz, "Observations and measurements of the solar aureole," in *Preprint of the Third Conference on Atmospheric Radiation* (American Meteorological Society, Boston, Mass., 1978), pp. 238–240.
2. L. L. Holladay "The fundamentals of glare and visibility," J. Opt. Soc. Am. **12**, 271–308 (1926).
3. H. Schober, *Das Sehen* (Deuticke, Leipzig, 1954), Vol. 2, pp. 74–90, 268–274.
4. K.Uchikana and M. Ikeda, "Accuracy of measurements for brightness of colored lights measured with successive comparation method," J. Opt. Soc. Am. A **3**, 34–39 (1986).
5. F. E. Volz, "Strong decline near Boston of solar aureole brightness and column load of giant particles," J. Geophys. Res. (to be published).
6. S. K. Seilkopf and P. L. Finkelstein, "Acid precipitation pattern and trends in eastern North America, 1980–1984," J. Clim. Appl. Meteorol. **26**, 980–994 (1987).
7. S. L. K. Briggs, "Trends in fine and coarse aerosol concentrations from 1979 to 1986 in six U.S. cities," in *PM-10, Implementation of Standards*, C. V. Mathai and D. H. Stonefield, eds. (Air Pollution Control Association, Pittsburgh, Pa., 1988), pp. 191–206.
8. S. A. Changnon, "Historical atmospheric transmission changes and changes in midwestern air pollution," Bull. Am. Meteorol. Soc. **68**, 477–480 (1978).
9. "Total suspended particulates trend analysis 1973–1983," in *DAQC Information Systems* (Massachusetts Department of Environmental Quality Engineering, Boston, Mass., 1985), pp. 13–20.
10. C. E. Rodes, D. M. Holland, L. J. Purdue, and K. A. Rheme, "A field comparison of PM10 inlets at four locations," J. Air Pollut. Control Assoc. **35**, 345–354 (1985).
11. J. D. Chazin, "Justification for retention of the 24-hour TSP standard," in *PM-10, Implementation of Standards*, C. V. Mathai and D. H. Stonefield, eds. (Air Pollution Control Association, Pittsburgh, Pa., 1988), pp. 72–84.
12. Raw data reports, Environmental Protection Agency, Aerometric Information Retrieval System Air Quality Subsystem (National Computer Center, Research Triangle Park, N.C., 1986–1990).
13. K. E. Noll and M. J. Pilat, "Size distribution of atmospheric giant particles," Atmos. Environ. **5**, 527–540 (1971).
14. K. E. Noll, A. Pontius, R. Frey, and M. Gould. "Comparison of atmospheric coarse particles at an urban and non-urban site," Atmos. Environ. **19**, 1931–1943 (1985).
15. K. T. Whitby, "The physical characteristics of sulfur aerosols," Atmos. Environ. **12**, 135–159 (1978).
16. K. E. Noll, R. Draftz, and K. Y. P. Fang, "The composition of atmospheric coarse particles at an urban and non-urban site," Atmos. Environ. **21**, 2717–2721 (1987).
17. D. A. Lundgren and H. J. Paulus, "The mass distribution of large atmospheric particles," J. Air Pollut. Control Assoc. **25**, 1227–1231 (1975).
18. Y. Mamane and K. E. Noll, "Characterization of large particles at a rural site in the eastern United States: mass distribution and individual particle analysis," Atmos. Environ. **19**, 611–622 (1985).
19. V. P. Hobbs, D. A. Bowdle, and L. F. Radke, "Particles in the lower troposphere over the High Plains of the United States, Part I," J. Clim. Appl. Meteorol. **24**, 1344–1356 (1985).
20. F. W. P. Götz, "Kontraständerungen flächenhafter Himmelsobjekte infolge der Lichtzerstreuung in der Erdatmosphäre," Astron. Nachr. **213**, 65–72 (1921).
21. F. E. Volz, "Optik des Dunstes," in *Handbuch der Geophysik*. F. Linke and F. Moller, eds. (Bornträger, Berlin, 1956), Vol. 8., pp. 888–892.
22. R. Eiden, "The influence of the size of the Sun on the sky light distribution," Appl. Opt. **7**, 1648–1649 (1968).
23. M. A. Box and A. Deepak, "Finite Sun effect on the interpretation of solar aureole," Appl. Opt. **20**, 2806–2810 (1981).
24. M. Shiobara, T. Hayasaka, T. Nakajima, and M. Tanaka, "Aerosol monitoring using a spectral radiometer in Sendai, Japan," J. Meteorol. Soc. Jpn. **69**, 57–70 (1991).
25. F. E. Volz, "Measurements of the skylight scattering function," Appl. Opt. **26**, 4098–4105 (1978).
26. S. Günther, "Die Himmelshelligkeit in der Nähe der Sonne," Optik **5**, 240–257 (1949).